



# Investigation into the synergistic effects in ternary cementitious systems containing portland cement, fly ash and silica fume

Mateusz Radlinski<sup>a,\*</sup>, Jan Olek<sup>b,1</sup>

<sup>a</sup> Exponent Failure Analysis Associates, 149 Commonwealth Drive, Menlo Park, CA 94025, United States

<sup>b</sup> Purdue University, School of Civil Engineering, 550 Stadium Mall Drive, West Lafayette, IN 47907, United States

## ARTICLE INFO

### Article history:

Received 25 June 2010

Received in revised form 21 November 2011

Accepted 23 November 2011

Available online 30 November 2011

### Keywords:

Fly ash

Packing density

Ternary mixture

Silica fume

Synergistic effect

## ABSTRACT

This research was primarily conducted to verify the presence of synergistic effects in ternary cementitious systems containing portland cement (OPC), class C fly ash (FA) and silica fume (SF). A subsequent objective of the study was to quantify the magnitude of the synergy and to determine its source. For a ternary mixture containing 20% FA and 5% SF by mass, the synergistic effect was observed mostly at later ages (7 days onward) and it resulted in an increased compressive strength and resistance to chloride ion penetration as well as a reduced rate of water absorption (sorptivity) compared to predictions based on individual effects of FA and SF in respective binary systems. The observed synergy was attributed to both chemical and physical effects. The chemical effect manifested itself in the form of an increased amount of hydration products. The physical effect associated with packing density was, somewhat contrary to general belief, not due to an optimized particle size distribution of the binder components of the ternary cementitious system. Instead, it was the result of smaller initial inter-particle spacing caused by lower specific gravities of both FA and SF which, in turn, led to a lower volumetric w/cm. If the mixture design was adjusted to account for these differences, the physical effect would be diminished.

© 2011 Elsevier Ltd. All rights reserved.

## 1. Introduction

An increasing interest in the utilization of ternary OPC/FA/SF mixtures is a direct result of their excellent performance, which has been frequently attributed to synergistic effects taking place between fly ash and silica fume. The synergy can be described in two different ways. The first type of synergy is rather intuitive and its basic principle is that, when combined in a ternary system, FA compensates for deficiencies of SF, and vice versa, SF compensates for deficiencies of FA [1]. However, the “classical” definition of the term “synergy” describes it as the “interaction of two or more agents or forces so that their combined effect is greater than the sum of their individual effects” [2].

Some of the previously published data suggests the existence of synergistic effects (according to the above classical definition) in ternary systems with respect to compressive strength [3,4], permeation-related properties [5], plastic shrinkage cracking and chloride ion penetrability [6], sulfate resistance [7] and alkali-silica reaction [8,9]. However, there seems to be a disagreement regarding the source of this synergy, i.e., whether it is associated with

chemical effects, physical effects or both. Lilkov et al. [10] showed that, due to chemical interaction of fly ash and silica fume in the ternary system, the synergy manifested itself in the increased amount of hydration products and in the decreased amount of calcium hydroxide observed at an early age (within the first 24 h). Further, Weng et al. [11] reported a significant increase in the formation of hydration products between 3 and 7 days in a ternary system containing 10% SF and 30% FA.

On the other hand, Kwan and Wong [12] reported that ternary OPC/FA/SF mixtures possess a higher packing density than binary mixtures, thereby providing an indirect proof to synergy arising from the physical effects. Similarly, Popovics [4] suggested that the improvement in workability observed for the ternary mixtures studied was a result of a more optimal (i.e., less “gap-graded”) particle size distribution. Yet, the data reported by Isaia [3] indicated that both the physical and the chemical synergistic effects were present in the investigated ternary systems incorporating fly ash and silica fume. The physical effect was presumably due to a higher content of particles smaller than 5  $\mu\text{m}$ , whereas the chemical effect was associated with higher pozzolanic activity of the ternary system, both of which were well reflected by an increased compressive strength.

It was clear from the literature review that the previous research dealing with the issues concerning synergistic effects in ternary systems was not “holistic”. Generally, the focus was either on the

\* Corresponding author. Tel.: +1 650 688 6752; fax: +1 650 328 3094.

E-mail addresses: [mrادلinski@exponent.com](mailto:mrادلinski@exponent.com) (M. Radlinski), [olek@purdue.edu](mailto:olek@purdue.edu) (J. Olek).

<sup>1</sup> Tel.: +1 765 494 5015.

physical or on the chemical aspect, or on evaluation of the impact of synergy on certain properties of ternary mixtures. Therefore, the present study was undertaken with three distinct objectives. The first objective was to verify whether synergistic effects (according to the “classical” definition) exist in a ternary cementitious system, in which silica fume and moderate amounts of class C fly ash are incorporated. Such moderate (15–25% by the total mass of the binder) fly ash contents have been frequently used in ternary mixtures evaluated by researchers and are common in field applications. Although differences exist between class C and class F fly ash (most notably higher reactivity typically exhibited by class C fly ash due to both pozzolanic and hydraulic properties) this study was limited to class C fly ash. This is, in part, due to local fly ash availability, and the fact that in majority of the above mentioned literature studies class F fly ash was usually incorporated. If the existence of the synergy was successfully confirmed, the subsequent objectives of this research were to quantify the magnitude of the synergy, and to examine whether the synergy is of a physical nature, a chemical nature, or both. To accomplish the above goals, a series of experiments was conducted, as broadly described in the following sections.

## 2. Experimental details

### 2.1. Materials

Ordinary ASTM C 150 Type I portland cement (OPC), class C fly ash (FA) meeting the requirements of ASTM C 618 and dry silica fume (SF) were used. In field applications, typically densified silica fume is used due to more economical transportation stemming from increased bulk density compared to undensified silica fume, and due to health concerns related to handling fine undensified silica fume particles. However, it was reported that densified SF particles undergo agglomeration [13,14], and thus they cannot be easily dispersed, particularly in paste mixtures, unless an ultrasound technique is applied [15]. Accordingly, in this study it was decided to use densified SF in mortar mixtures and undensified silica fume in pastes. Table 1 summarizes the chemical composition

and physical properties of the cementitious materials used in the study as provided by their suppliers.

Mortar mixtures incorporated siliceous sand with a fineness modulus of 3.7. To ensure satisfactory workability of mortar mixtures, approximately 2340 ml/m<sup>3</sup> of polycarboxylate high range water reducing admixture (HRWRA) was used in each mixture. HRWRA was not used in paste mixtures.

### 2.2. Mixture proportions and preparation

The following four types of binder systems were used in this study: plain cement mixture (OPC), binary mixture with 20% fly ash (20FA), binary mixture containing 5% silica fume (5SF) and ternary mixture with 20% fly ash and 5% silica fume (20FA/5SF). In each case, the cementitious materials (FA and SF) were used to replace a given percentage of cement (based on the total mass of the binder). These binder systems were used to prepare both the paste and mortar mixtures, each at a constant water-to-cementitious materials ratio (w/cm) of 0.41 by mass. All mortar mixtures were prepared with a paste content of 35.5% by volume. The detailed proportions of mortar mixtures are provided in Table 2.

Both the paste and the mortar mixtures were prepared using a laboratory Hobart-type mixer following the procedures of ASTM C 305. Paste specimens were made for compressive strength, thermogravimetric analysis (TGA) and isothermal calorimetry. Initially, paste specimens were also prepared for use in the rapid chloride permeability (RCP) and sorptivity tests. However, since paste sorptivity specimens developed extensive shrinkage cracking during conditioning, it was decided to conduct both the RCP and the sorptivity tests using mortar specimens.

### 2.3. Test procedures

For each part of this study, a distinct set of tests, each believed to be most suitable for achieving the previously stated objectives, was performed. The entire test matrix is summarized in Table 3.

**Table 1**  
Physical properties and chemical composition of cementitious materials used in study on synergistic effect (as reported by the suppliers).

Property	Cement	Class C fly ash	Silica fume
<i>Physical</i>			
Specific gravity	3.15	2.56	2.20
Fineness			
Retained on #325 mesh	–	20.4	–
Blaine's surface area (cm <sup>2</sup> /g)	3470	–	–
Compressive strength tested on mortar cubes (MPa)			
1 day	16.5	–	–
3 day	26.0	–	–
7 day	32.2	–	–
28 day	–	–	–
Strength activity index with portland cement at 7 days, % of cement control	–	97	–
<i>Chemical</i>			
Silicon dioxide SiO <sub>2</sub> (%)	20.04	41.40	93.07
Aluminum oxide Al <sub>2</sub> O <sub>3</sub> (%)	5.84	19.98	0.62
Ferric oxide Fe <sub>2</sub> O <sub>3</sub> (%)	2.28	5.95	0.41
Calcium oxide CaO (%)	64.87	16.23	0.66
Magnesium oxide MgO (%)	1.63	3.72	1.16
Sulfur trioxide SO <sub>3</sub> (%)	3.28	0.99	<0.01
Loss on ignition (%)	1.13	1.05	2.71
Sodium oxide Na <sub>2</sub> O (%)	0.14	–	–
Potassium oxide K <sub>2</sub> O (%)	0.88	–	–
Total alkali as sodium oxide Na <sub>2</sub> O (%)	0.72	2.46	0.67
Insoluble residue (%)	0.47	–	–
<i>Potential compound composition (Bogue)</i>			
Tricalcium silicate C <sub>3</sub> S (%)	60	–	–
Dicalcium silicate C <sub>2</sub> S (%)	12	–	–
Tricalcium aluminate C <sub>3</sub> A (%)	12	–	–
Tetracalcium aluminoferrite C <sub>4</sub> AF (%)	7	–	–

**Table 2**  
Mixture composition of mortar mixtures.

Mix designation	OPC	20FA	5SF	20FA/5SF
Water-cementitious				
Materials ratio	0.41	0.41	0.41	0.41
Paste (%)	35.5	35.5	35.5	35.5
Cement (kg/m <sup>3</sup> )	455	357	428	332
Fly ash (kg/m <sup>3</sup> )	0	89	0	89
Silica fume (kg/m <sup>3</sup> )	0	0	23	22
Fine agg. (SSD) (kg/m <sup>3</sup> )	1590	1590	1590	1590
Water (kg/m <sup>3</sup> )	187	183	185	182
HRWRA – avg. (ml/m <sup>3</sup> )	2370	2330	2350	2310

All specimens designated as 180 days old equivalent were obtained by using the following accelerated curing procedure: 0–7 days moist curing at 23 °C; 7–56 days moist curing at 38 °C. Based on data recently published by Bognacki et al. [16], it was assumed that by the 56th day the specimens subjected to accelerated curing had reached a maturity level equivalent to at least 180 days of continuous curing at 23 °C. For simplicity, these specimens will be thereafter referred to as 180 days specimens.

During the first portion of the study consisting of verification of synergistic effects, compressive strength, resistance to chloride ion penetration and water sorptivity were evaluated. Compressive strength tests were conducted at the ages of 0.5, 1, 3, 7, 28 and 180 days according to ASTM C 109 on a set of three 51 × 51 × 51 mm paste specimens. The resistance to chloride ion penetration was evaluated on mortar specimens using ASTM C 1202 “rapid chloride permeability” (RCP) test. The test output is the total charge (in coulombs) passed through the specimen across which a 60 V potential is applied for 6 h. Despite certain limitations of the RCP test [17,18], the test results have been found to correlate well with the coefficient of chloride diffusion of concrete [19–21]. Two replicate cylindrical (51 × 102 mm) specimens from each mixture were tested at ages of 7, 28 and 180 days.

The water sorptivity test was performed using a modification of the standard ASTM C 1585 rate of water absorption test. The test specimens consisted of two replicate mortar cylinders, each measuring 51 × 102 mm. Following the specified length of moist curing, i.e., 7, 28 or 180 days, all specimens were dried at 23 °C and 50% RH for 14 days. Subsequently, they were subjected to the standard (ASTM C 1585) conditioning procedure. Accordingly, the specimens were placed for 3 days in a desiccator which was stored inside the oven set at 50 °C. The relative humidity (RH) inside of the desiccator was maintained at 80% by means of a saturated solution of potassium bromide. After 3 days, the specimens were removed from the desiccator and stored individually in well-sealed plastic containers for 14 days at room temperature (23 °C). Next, the perimeter of each specimen was coated with epoxy. Also, a dike was formed on top of the specimens using aluminum tape and silicone caulk, whereas the bottom was covered with a polyethylene sheet secured with a rubber band. Tap water was then placed in a dike and the water intake was determined by weighing the specimens upon removal of water from the top the specimens at the specific time intervals described in ASTM C 1585. The mass of

water gained divided by the cross-sectional area of the specimens and density of water was plotted against the square root of time. Such an analysis gives two distinct lines. The slope of the line for the data collected during the time interval from 0 to 6 h is called initial sorptivity and it represents the rate of capillary-driven water absorption. The slope of the second line for the data collected from day 1 to day 8 is referred to as secondary sorptivity and it generally reflects other phenomena besides the capillary forces alone, such as filling of the larger pores and air voids [22]. Accordingly, the results of the secondary sorptivity test were not included in this paper as they may not accurately reflect hydration-related microstructural changes in the evaluated cementitious systems.

The second set of tests was carried out to evaluate the chemical reactivity of the binder components in the mixtures studied. Accordingly, isothermal calorimetry was conducted to gain knowledge about the rate of reactivity (signified by the rate of heat evolved) at early ages, whereas thermogravimetric analysis (TGA) was conducted to determine the extent of hydration at both early and late ages. Isothermal calorimetry was conducted using a JAF Isothermal Conduction Calorimeter manufactured by Wexham Developments®. Paste specimens were tested in a “large sample” (nominally 30 g of cementitious materials) configuration at a constant temperature of 21 °C. Two replicate samples were tested concurrently and the average output was reported. The experiment was terminated after the output voltage had dropped to negligible values (after about 90–120 h). Immediately after completion of the experiment, each specimen was subjected to a calibration procedure in order to determine calorimeter constants from the Tian-Calvet equation, as broadly described in the operating manual [23].

Thermogravimetric analysis was performed using a TGA 2050 Thermogravimetric Analyzer manufactured by TA Instruments. At the age of 0.5, 1, 3, 7, 28 and 180 days, several small (approximately 1 cm<sup>3</sup>) pieces of paste were chipped off the interior of a cubical (51 × 51 × 51 mm) specimen which was previously subjected to compressive strength testing. To cease the hydration process, the pieces were immediately soaked in acetone for a period of about 14 days (acetone was changed after 7 days). Prior to testing, the pieces were ground using mortar and pestle until all material passed a #200 (75 µm) sieve. A sample of about 40 mg was then placed in the instrument sample holder and the testing was initiated. The automatic two-step testing procedure was used. In the first step, the instrument maintained isothermal conditions for the first 10 min (to allow for equilibration of specimen weight). This was followed by heating to 1000 °C at a rate of 10 °C/min. Generally, two specimens were used for TGA. However, if the difference in test results was excessive, a third specimen was tested.

### 3. Test results and discussion

#### 3.1. Verification of existence of synergistic effects in OPC/FA/SF systems

The results of compressive strength, rapid chloride permeability and initial sorptivity tests are shown in Fig. 1 through Fig. 3, respectively. Each figure contains data for the four mixtures

**Table 3**  
Test matrix.

Specimen type	Purpose of the test				
	Verification of existence and quantification of magnitude of synergistic effect			Examination of chemical nature of synergy	
	Compressive strength (0.5, 1, 3, 7, 28, 180°d)	RCP (7, 28, 180°d)	Sorptivity (7, 28, 180°d)	Thermogravimetric analysis	Isothermal calorimetry
Paste	✓			✓	✓
Mortar		✓	✓		

Note: °d designates a 180 days equivalent age obtained using accelerated curing procedure: 0–7 days at 23 °C, 7–56 days at 38 °C.

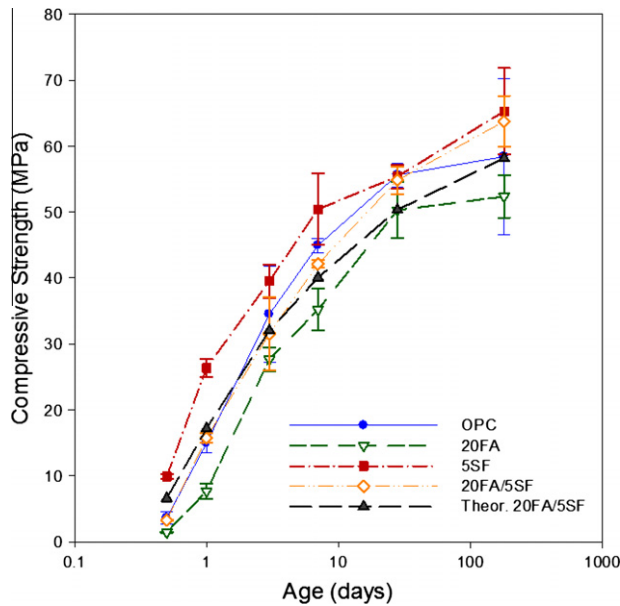


Fig. 1. Compressive strength results (paste specimens).

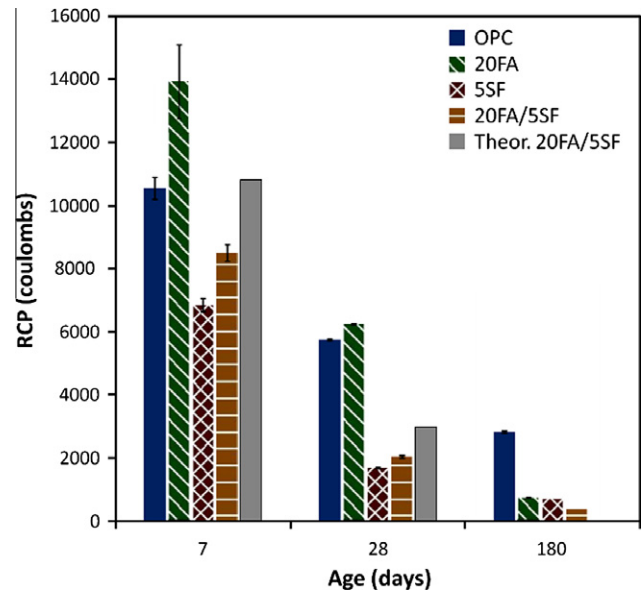


Fig. 2. RCP test results (mortar specimens).

studied, as well as the theoretical (i.e., predicted) value of a given property for the 20FA/5SF ternary system. The theoretical value of any predicted property (labeled as  $P_{Theor.20FA/5SF}$ ) was approximated using the following equation:

$$P_{Theor.20FA/5SF} = P_{OPC} + 0.95\Delta P_{20FA} + 0.80\Delta P_{5SF} \\ = P_{OPC} + 0.95(P_{20FA} - P_{OPC}) + 0.80(P_{5SF} - P_{OPC}) \quad (1)$$

where  $P_{OPC}$ ,  $P_{20FA}$ ,  $P_{5SF}$  are the values of a given property for OPC, 20FA, and 5SF mixtures, respectively. Eq. (1) represent a formula proposed by Thomas et al. [9] modified by incorporating coefficients 0.95 and 0.80 which represent the sum of volume fractions of, respectively, OPC (0.75) and FA (0.20) associated with the binary 20FA mixture, and OPC (0.75) and SF (0.05) associated with the binary 5SF mixture, in the ternary 20FA/5SF system.

### 3.1.1. Compressive strength

The compressive strength curves for the binary mixtures containing either 20% fly ash or 5% silica fume comprise, respectively, the lower and the upper boundaries of all the compressive strength data shown in Fig. 1. The early-age (up to 3 days) strength of the ternary 20FA/5SF mixture was lower than the theoretical values predicted using Eq. (1). However, at 28 and 180 days the ternary mixture developed strength that was practically identical to the strength of the 5SF mixture and notably higher than predicted values. This implies that, with respect to compressive strength, the synergistic effect does seem to exist in the ternary system containing fly ash and silica fume but becomes apparent only at later ages. This is likely due to the relatively low reactivity of the fly ash itself, as manifested by the 180-day compressive strength of the FA mixture being lower than that of the OPC mixture at the same age.

### 3.1.2. Resistance to chloride ion penetration

The resistance to chloride ion penetration of the mixtures evaluated using the RCP test is shown in Fig. 2. The 7-day and 28-day data exhibit trends similar to the compressive strength data (Fig. 1). Specifically, of all the mixtures studied, the binary mixture with 20% fly ash exhibited the lowest resistance to chloride ion penetration (highest RCP values), whereas the binary mixture with 5% SF showed the highest resistance (lowest RCP values). However, unlike in the case of compressive strength data, where the 20FA

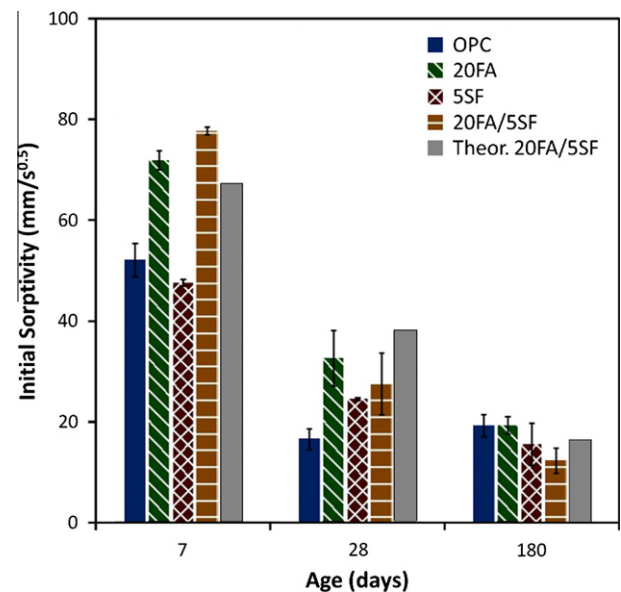


Fig. 3. Initial sorptivity data (mortar specimens).

mixture still showed the lowest strength at later age, the 180-day coulomb value of that mixture dropped to the same levels as observed for the 5SF mixture.

It was also observed that the RCP values of the ternary mixture were less affected by the presence of fly ash than their compressive strength values. Specifically, while the 7-day compressive strength of the 20FA/5SF mixture was approximately mid-way between the strength for the 20FA and 5SF mixtures (Fig. 1), the 7-day RCP of the ternary mixture was only slightly higher than that of the 5SF mixture (Fig. 2). Similarly, the 180-day strength of the 20FA/5SF mixture was lower than that of the 5SF mixture, whereas the ternary mixture had the lowest value (384 coulombs) of all the mixtures studied at 180 days. Most notably, with the exception of the 180-day RCP for which Eq. (1) returned a negative theoretical RCP value, the measured RCP values of the ternary mixture were lower than the theoretical values. This implies that the excellent resistance to chloride ion penetration observed for the ternary system



is at least partially attributable to the synergistic interaction taking place between fly ash and silica fume. It can be also seen that even at 180 days the OPC mixture still exhibited relatively high (about 3000 coulombs) values. This, in turn, demonstrates the general beneficial effect of the incorporation of mineral admixtures on long-term durability.

### 3.1.3. Initial sorptivity

The raw data from sorptivity tests, represented as a linear relationship between change in mass of specimens and square root of time collected from 0 to 6 h, were not included in the paper for brevity. Fig. 3 which shows the initial sorptivity coefficients determined at 7, 28 and 180 days reveals a somewhat unexpected outcome. While the OPC mixture was clearly outperformed by the 5SF and 20FA/5SF mixtures in the rapid chloride permeability test (Fig. 2), the initial sorptivity of the OPC mixture was generally comparable to that of the 5SF mixture. Interestingly, the ternary mixture had the highest initial sorptivity at 7 days, whereas at 28 days only the 20FA mixture displayed a higher initial sorptivity than the 20FA/5SF mixture. However, while at 180 days all mixtures performed comparably, the ternary mixture attained the lowest initial sorptivity. By comparing the measured and theoretical data for the ternary mixture, the synergistic effect with respect to initial rate of water absorption is visible at 28 and 180 days.

It should be pointed out, however, that regardless of the magnitude of the synergistic effect, the long-term performance of the ternary 20FA/5SF mixture appears very promising due to the highest strength and resistance to chloride ion penetration, as well as the lowest initial rate of water absorption developed by that mixture.

### 3.2. Quantification of synergistic effects

While the existence of synergistic effects was qualitatively demonstrated in the previous section, the purpose of the current section is to quantify the magnitude of those effects for each of the studied properties of the OPC/FA/SF mixture. The magnitude of the synergistic effect was calculated from the following formula:

$$SE = j \cdot \frac{P_{20FA/5SF} - P_{Theor.20FA/5SF}}{P_{Theor.20FA/5SF}} \times 100\% \quad (2)$$

where  $SE$  is the synergistic effect (%),  $P_{20FA/5SF}$  is a measured value of a given property for the 20FA/5SF mixture,  $P_{Theor.20FA/5SF}$  is a theoretical value of a given property for the 20FA/5SF mixture calculated from Eq. (1),  $j = 1$  for properties to be maximized (compressive strength) and  $j = -1$  for properties to be minimized (rapid chloride permeability and initial sorptivity). The above formula constitutes a minor modification of the formula previously implemented by Isaia [3], who calculated the synergistic effect with respect to the value of a property developed by the reference (i.e., OPC) mixture, rather than that of a theoretical 20FA/5SF mixture ( $P_{Theor.20FA/5SF}$ ).

The values of the synergistic effect for the evaluated properties are shown in Table 4. At the early ages (up to 3 or 7 days, depending on the property), the  $SE$  values are typically negative, implying lack of any synergistic effect. This, however, does not necessarily imply that the ternary mixture performed poorly. Quite the opposite, in almost all cases the 20FA/5SF mixture performed better than the 20FA mixture (which usually performed the worst). Nonetheless, at later ages the existence of synergy between fly ash and silica fume was very conspicuous, as  $SE$  values became positive and frequently exceeded 20%.

### 3.3. Examination of the physical nature of synergistic effect

In general, there are two distinctive physical mechanisms of improvement of concrete properties resulting from replacing

**Table 4**

Variation in synergistic effect ( $SE$ ) values with age.

Age (days)	Value of synergistic effect $SE$ (%)		
	Compressive strength	RCP	Initial Sorptivity
0.5	−50.2	–	–
1	−8.4	–	–
3	−1.4	–	–
7	5.1	21.2	−15.5
28	8.9	31.0	27.9
180 <sup>a</sup>	9.6	n/a	24.4

Note: <sup>a</sup>designates a 180 days equivalent age obtained using accelerated curing procedure: 0–7 days at 23 °C, 7–56 days at 38 °C; n/a denotes a case where computation of the synergistic effect was not possible due to negative theoretical  $P_{Theor.20FA/5SF}$  value.

cement by fine pozzolanic material (particularly SF): higher volumetric concentration of solid binder components (due to optimized combined particle size distribution [4,12]), also referred to as the filling effect [24] and densification of interfacial transition zone (ITZ) [25]. Since the current study is focused on the synergistic effects present in ternary cementitious systems, including pastes, only the first source of physical action will be considered.

#### 3.3.1. Effect of binder composition on volumetric $W/CM$

Given that higher packing density of particles in a given unit volume of paste is beneficial with respect to improvement of properties of the ternary system studied, it should be realized that the mixtures containing either fly ash or silica fume (and especially both) were favored over the OPC mixture. This is because the mixtures were designed in a “standard” way, and thus the water-cementitious materials ratio was not adjusted for the lower specific gravities of FA and SF compared to cement (Table 1). As a result, the volumetric water-cementitious materials ratio was lower in the case of mixtures containing FA and SF. Although the differences in the resulting volumetric  $w/cm$  do not appear to be significant (1.292, 1.235, 1.264 and 1.210 for OPC, 20FA, 5SF, 20FA/5SF mixtures, respectively), they actually translate into quite pronounced differences in  $w/cm$  (by mass) that the mixtures containing FA and SF should be designed with in order to match a  $w/cm$  of 0.41 of the OPC mixture, i.e., 0.429 for 20FA, 0.419 for 5SF, and 0.438 for the 20FA/5SF mixture.

#### 3.3.2. Packing density

Recently, Wong and Kwan [24] demonstrated that there exists an optimum  $w/cm$  at which maximum packing density (minimum voids ratio) occurs in mixtures containing FA or SF. This approach allows one to increase the density of paste by optimizing the composition of the cementitious system and varying the  $w/cm$ . When extended to ternary mixtures with FA and SF [12], it was found that these mixtures possessed higher packing density than their counterpart binary mixtures. However, these authors also showed that no improvement in packing of the particles should be expected in pastes with a volumetric  $w/cm$  higher than about 0.70 (Fig. 4). This is signified by a convergence of the voids ratio- $w/cm$  curves for plain OPC, 25FA and 15SF mixtures and the data points falling on the diagonal line, which represents the equality of volumetric  $w/cm$  and voids ratio. Accordingly, irrespective of binder composition, above a volumetric  $w/cm$  of 0.70 the particles are dispersed to the point that the mixture becomes a suspension of granular particles in water.

It is important to recognize that a volumetric ratio of 0.70 translates into  $w/cm$  by mass of about 0.23. Such a low water-cementitious materials ratio is certainly not feasible in typical high performance concrete applications, and may perhaps be only encountered in ultra high performance concrete (UHPC) (see, for

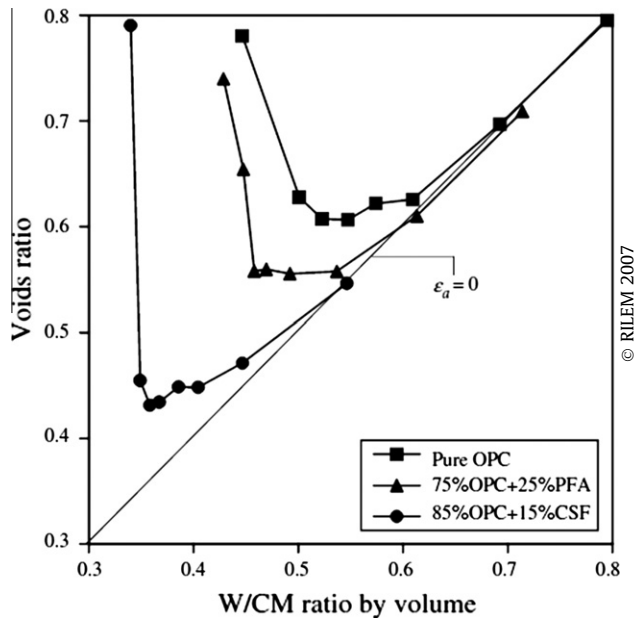


Fig. 4. Relationship between voids ratio and w/cm ratio by volume (from [24]; with kind permission from Springer Science + Business Media: Materials and Structures, packing density of cementitious materials: part 1—measurement using a wet packing method, vol. 41(4), 2008, p. 698, Wong HCW, and Kwan AKH. Fig. 6).

example, Refs. [26,27]). Thus, it appears that an enhancement in certain properties of conventional (i.e., not UHPC) concrete containing fly ash and silica fume may not be, as previously suggested [3,4], due to a more densely packed cementitious system resulting from an optimized particle size distribution of binder components. Instead, the observed densification of the binder may be attributed to differences in the specific gravities of these materials, as discussed in Section 3.3.1.

### 3.4. Examination of chemical nature of synergistic effect

#### 3.4.1. Isothermal conduction calorimetry

The rate of heat evolution during the initial hydration stage obtained from isothermal calorimetry is presented in Fig. 5. To preserve clarity, only one curve per mixture is shown since the individual curves for the two replicate samples prepared from a given mixture were nearly perfectly overlapping. As expected, incorporation of silica fume in the binary (5SF) mixture had an accelerating effect, whereas the presence of fly ash (mixture 20FA) had a retarding effect. Accordingly, the heat evolution peak for the 5SF mixture is slightly shifted to the left and is significantly higher (by about 0.5 W/kg) compared to the OPC mixture. Analogously, due to a longer dormant period, the peak for the 20FA mixture is shifted to the right (with respect to OPC peak) and is lower by about 0.5 W/kg. The heat evolution rate curve for the ternary system is located between those for the binary mixtures with either FA or SF. However, clearly due to inclusion of FA, the initial rate of reaction observed in the ternary system was hampered compared to the OPC mixture.

Table 5 provides a comparison of the maximum heat evolution rates derived from Fig. 5. It can be seen that after the data have been normalized by cement content, the binary and ternary mixtures exhibited higher rates than the OPC mixture. This implies that in the presence of either fly ash or silica fume, the early stage of hydration of cement is increased, as previously reported by Ballim and Graham [28]. This accelerating effect is much more

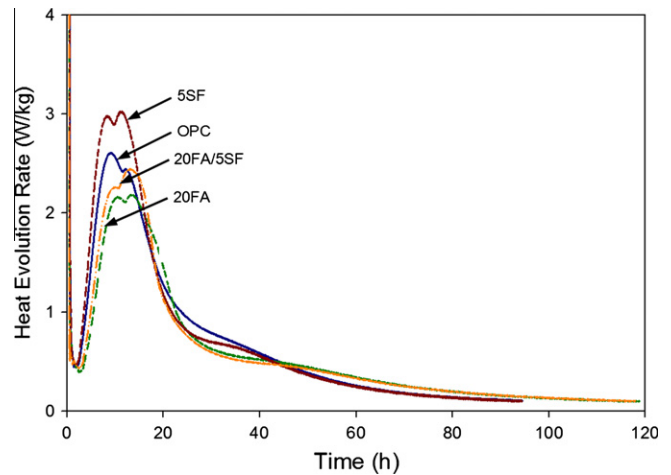


Fig. 5. Heat evolution rate from isothermal calorimetry expressed as W per kg of binder.

pronounced for the 5SF mixture than for the 20FA mixture, whereas it is clearly magnified for the ternary 20FA/5SF mixture.

The current data appear somewhat inconsistent with the findings of Nocuń-Nocuń-Wczelik [29], who reported that the rate of heat evolution of the mixtures containing 20% FA was only slightly lower than that of the plain cement mixture, whereas the ternary mixture with 20% FA and 10% SF exhibited much more depressed rates of heat development. These discrepancies can be explained by the use of different types of fly ash and, more importantly, by preparation of the mixtures at a w/cm of 0.50 (as opposed to 0.41 used in the present study).

Another important implication of the data presented in Fig. 5 is that, although the maximum temperature rise due to hydration for the ternary system may be higher than that observed for the mixture containing fly ash only, it may be still below the maximum temperature of the OPC mixture. This would be very advantageous from the standpoint of a reduction of the thermal stresses (absolute or differential) generated due to thermal contraction upon cooling of the structure. However, further work is needed to verify this hypothesis under adiabatic or semi-adiabatic conditions.

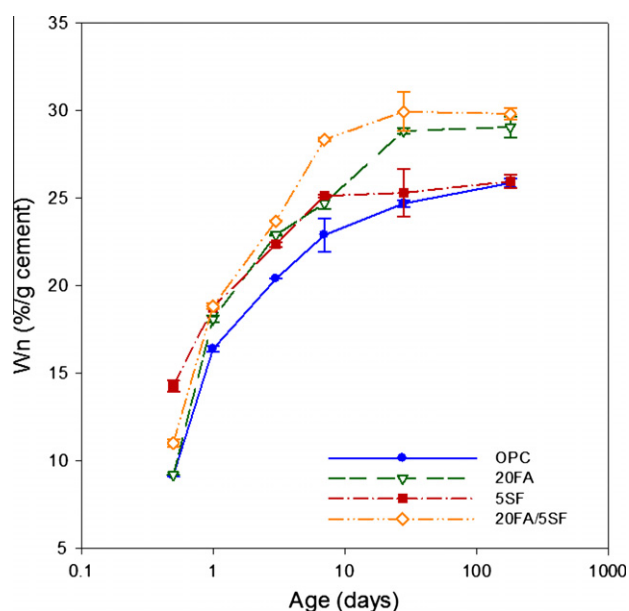
In summary, since the synergistic effect was not observed for the 20FA/5SF system at the early age (Table 4), isothermal calorimetry did not successfully confirm the chemical nature of the synergy, as it provides information about the rates of chemical reactions occurring exclusively during the early-age period.

#### 3.4.2. Thermogravimetric analysis

To more completely evaluate the chemical reactions taking place in the mixtures over the course of hydration (i.e., at both early and late ages), thermogravimetric analysis of hydrated pastes was performed. The variation in total non-evaporable water content  $W_n$  derived from the differences in sample mass at 105 °C and 950 °C is shown in Fig. 6. The results are presented as a percentage of weight of anhydrous cement, which provides a clearer illustration of changes occurring due to the presence of mineral admixtures [30]. It can be seen that already within the first 12 h the reactions in the 5SF mixture progressed much faster than in the plain cement mixture. Conversely, the 20FA mixture showed an amount of hydration products comparable to the OPC mixture, whereas for the ternary mixture the amount of non-evaporable water was only slightly higher than for the OPC mixture. However, at 1 day the amount of hydration products (expressed by weight of cement) was comparable in the ternary and binary mixtures. Interestingly, at 28 and 180 days the non-evaporable water content of

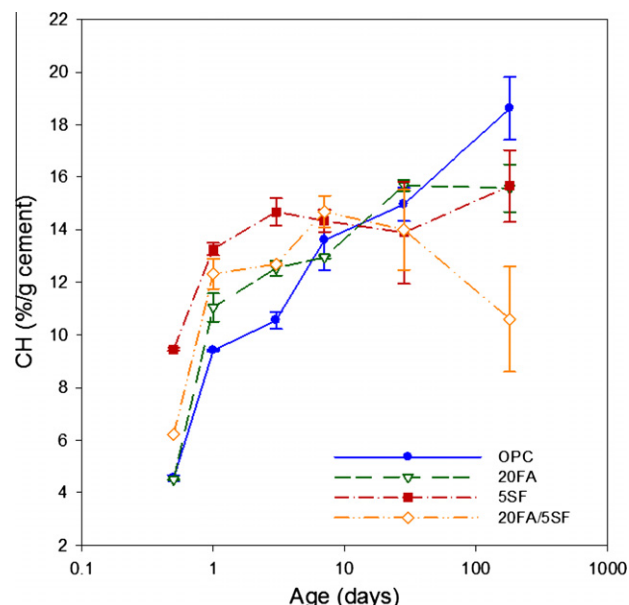
**Table 5**Comparison of maximum heat evolution rate ( $dQ/dt$ ).

Mixture	Max. $dQ/dt$ (W/kg of total cementitious materials)	Max. $dQ/dt$ (W/kg of cement)
OPC	2.60	2.60
20FA	2.18	2.72
5SF	3.02	3.18
20FA/5SF	2.44	3.25

**Fig. 6.** Changes in the non-evaporable water content ( $W_n$ ) with hydration time.

5SF was similar to that of the plain cement mixture. On the other hand, a substantial increase in  $W_n$  was observed at 7 days for the 20FA/5SF mixture and at 28 days for the 20FA mixture. It should be noted that the  $W_n$  measurements, particularly at the later age, for mixtures containing silica fume or fly ash are likely deflated due to polymerization of silica [31,32]. This phenomenon results in conversion of the previously chemically bound non-evaporable water to evaporable water and thus lowers the TGA measurements of  $W_n$ .

Fig. 7 shows the variation in calcium hydroxide (CH) computed from sample mass loss at about 450 °C. This temperature signifies loss of water due to decomposition of calcium hydroxide into calcium oxide and water. Again, to demonstrate the effect of pozzolanic reactions more clearly, the CH amount is expressed as percent by weight of anhydrous cement. The initial upsurge in the amount of CH produced observed for the 5SF mixture (Fig. 7) is likely attributed to accelerated hydration of the cement itself [33]. The drop in CH content due to the pozzolanic reaction is observed only after 3 days, which is in agreement with findings of Zelić et al. [34]. However, likely due to depletion of silica fume available for pozzolanic reaction with CH, the CH content increased again between 28 and 180 days, while still remaining well below the CH level found in the plain OPC mixture at 180 days. These results contradict the data reported by Weng et al. [11], who observed lower (by 3–5%) CH content at all testing ages for a mixture containing 5% SF prepared at a w/cm of 0.40, as compared to the plain cement mixture. This difference can be perhaps attributed to the use of silica fume in undensified form in the present study. When used in this form, it could possibly provide more nucleation sites and thus enhanced

**Fig. 7.** Variation in calcium hydroxide (CH) content with hydration time.

early age cement hydration [34], thereby increasing the amount of CH produced. However, due to lack of information regarding the form of SF used by the above authors, this conclusion is purely hypothetical.

At 1 and 3 days, the CH content for the 20FA mixture was higher than that for the OPC mixture (Fig. 7). This implies that, much like silica fume, fly ash accelerated the early age cement hydration. This acceleration might be due to dissolution of alkali (i.e.,  $K_2O$ ) from some fly ash particles into the paste at early age [35] or due to the “dilution effect” reportedly occurring as a result of a higher amount of water available for hydration of cement caused by low initial reactivity of fly ash itself [3,28]. While the comparable CH content of 20FA and OPC mixtures at 7 and 28 days may be viewed as an indication of the relative inertness of fly ash, it is misleading since the 20FA mixture produced in fact more gel than the plain cement mixture at each respective age (Fig. 6). At 180 days, a significant reduction in CH content was observed for the 20FA mixture and the resulting amount of CH was the same as in the 5SF mixture.

The amount of calcium hydroxide found in the 20FA/5SF mixture at early age was between that for the 20FA and 5SF mixtures. A moderate drop in CH content occurred between 7 and 28 days, whereas the final (180-day) CH amount for the ternary mixture was only about 10.5%. This implies that, while this amount is significantly less than the CH content of the OPC mixture (18.5%) or the binary mixtures (about 15.5%), more SCMs (preferably FA) could be incorporated in the ternary system to further reduce the CH content.

Hydration of cement and pozzolanic reactions with either fly ash or silica fume are simultaneously ongoing processes in which cement increases both the amount of CH and  $W_n$ , whereas FA and SF reduce CH and may increase or decrease  $W_n$ . However, this situation is further complicated by different (i.e., typically higher) cement hydration rates in the presence of mineral admixtures compared to those in a plain cement system and by the fact that class C fly ash possesses certain hydraulic properties [30]. Hence, it is not possible to simply separate the effects of these two reactions and infer from either  $W_n$  or CH contents how much of each component of the system has reacted. Instead, a concept of “hydrate water” [10,11,30] can be utilized to assess the total amount

of silicate gel products (calcium silicate hydrate (C-S-H) and calcium silica-alumina hydrate (C-AS-H)). This quantity can be estimated by subtracting the amount of water associated with calcium hydroxide from the total non-evaporable water content, as follows:

$$W_H = W_n - W_{CH} \quad (3)$$

where  $W_H$  is hydrate water,  $W_n$  is non-evaporable water and  $W_{CH}$  is water associated with dehydration of CH. It should be noted that this approach provides only an estimate of the silicate gel products, as it does not account for different stoichiometry, molar volume and water content of C-S-H produced from cement hydration in absence of mineral admixtures, from cement hydration in the presence of silica fume [36] and from pozzolanic reactions of FA and SF with CH [37].

The variation in hydrate water with time is shown in Fig. 8. As expected, the binary mixtures containing either fly ash or silica fume had an increased amount of hydrate water (normalized by weight of anhydrous cement) compared to the plain cement mixture. Also, not surprisingly, with exception of the 12-h data, the  $W_H$  content for the ternary mixture was higher than that observed for any other mixture. However, at the early ages (12 h to 3 days) the amount of hydrate water found in the 20FA/5SF mixture was lower than the theoretical amount predicted using Eq. (1). In contrast, at later ages (7–180 days) the measured values of  $W_H$  were higher than theoretical values, which gives rise to a chemical-based synergistic effect. These findings appear to reflect fairly well the trends observed for most of the properties evaluated (Table 4), where the  $SE$  values were typically negative at the early age and positive at the later ages. It should be kept in mind that the aforementioned artifact of reduced  $W_n$  quantities measured using the TGA technique resulting from polymerization of silica in the mixtures containing silica fume or fly ash also directly impacted the  $W_H$  values for those mixtures. However, it is reasonable to assume that the binary (5SF and 20FA) mixtures and the ternary 20FA/5SF mixture were affected by this phenomenon proportionally to the silica content (from either silica fume or fly ash) in those mixtures. It follows that, based on Eq. (1), the relative ratio of measured  $W_H$  for a 20FA/5SF mixture to the corresponding theoretical value would be the same. Accordingly, the magnitude of synergistic effect associated with  $W_H$  can also be assumed to remain unchanged.

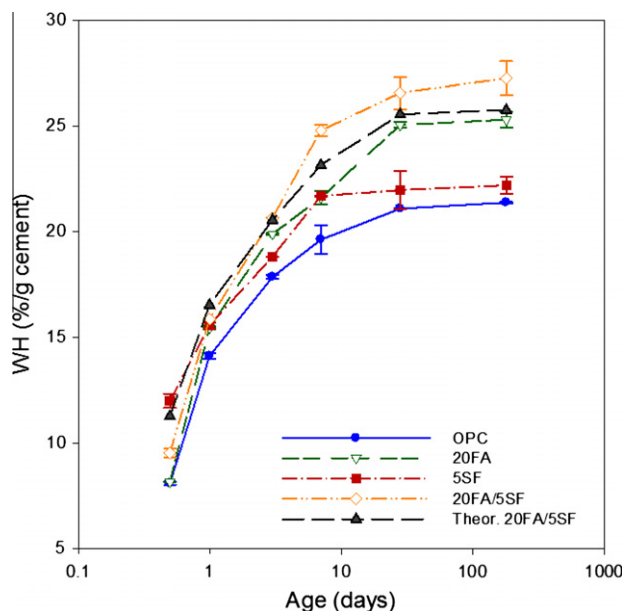


Fig. 8. Variation in hydrate water content ( $W_H$ ) with hydration time.

Based on the results of this study, it appears that the chemical effect related to formation of a higher volume of hydration products than theoretically predicted is, at least, partially responsible for the synergy observed for the properties evaluated. Although the differences between the predicted and measured  $W_H$  of the ternary mixture do not appear significant at later age (0.6–1.1%), the associated amount of hydration products is proportionally higher. For instance, a 1% increase in  $W_H$  may translate into about 0.13 g (or 0.05 cm<sup>3</sup>) more of C-S-H (with assumed chemical composition of  $C_{1.7}SH_4$  [38] and density of 2.44 g/cm<sup>3</sup> [39]) produced per 1 g of cement. Considering that at the high degree of hydration associated with later age, the pore system is already partially depercolated, such an increase may have a significant effect on transport-related properties. Further, the above differences represent only the additional benefit of incorporating fly ash and silica fume in the ternary system, beyond that predicted based on the effects of individual components.

#### 4. Conclusions

Synergistic effects reportedly taking place in ternary cementitious systems containing fly ash and silica fume were investigated in this study. This examination led to the following conclusions:

- For a ternary mixture containing 20% FA and 5% SF, the synergistic effect (according to classical definition) was observed mostly at later ages (7 days and onward).
- The synergy observed for the ternary OPC/FA/SF system was attributed to both chemical and physical effects.
- The chemical effect manifested itself in the form of an increased amount of hydration products compared to predictions based on the individual effects of fly ash and silica fume in the binary systems.
- The physical effect associated with packing density was somewhat contrary to general beliefs and appeared to have not been caused by optimized particle size distribution of binder components of the ternary cementitious system. Instead, it was a result of smaller initial inter-particle spacing resulting from lower specific gravity of both fly ash and silica fume, which led to lower volumetric w/cm. If the mixture design was adjusted to account for these differences, it is expected that the physical effect would be diminished.
- Since in addition to the presence of synergy (according to the “classical” definition) fly ash and silica fume mutually compensate for each other’s deficiencies (noticeable when they are used alone in a binary system), incorporation of ternary OPC/FA/SF cementitious systems is deemed to be beneficial.

#### Acknowledgment

The authors would like to acknowledge Tony Kojundic of Elkem Materials Inc. for providing silica fume for this research.

#### References

- [1] Thomas MDA, Bamforth PB. Modeling chloride diffusion in concrete effect of fly ash and slag. *Cem Concr Res* 1999;29(4):487–95.
- [2] The American heritage dictionary of the English language. 4th ed. Houghton Mifflin Company; 2006, from Dictionary.com [October 13, 2008]. <<http://dictionary.reference.com/browse/synergy>>.
- [3] Isaia GC. Synergic action of fly ash in ternary mixtures with silica fume and rice husk ash. In: Proceedings 10th international congress on the chemistry of cement, vol. 3. Gothenburg, Sweden; 1997.
- [4] Popovics S. Portland cement-fly ash-silica fume systems in concrete. *Adv Cem Based Mater* 1993;1(2):83–91.
- [5] Khan MI. Permeation of high performance concrete. *J Mater Civ Eng* 2003;15(1):84–92.



- [6] Bouzoubaâ N, Bilodeau A, Sivasundaram V, Fournier B, Golden DM. Development of ternary blends for high-performance concrete. *ACI Mater J* 2004;101(1):19–29.
- [7] Nehdi ML, Sumner J. Optimization of ternary cementitious mortar blends using factorial experimental plans. *Mater Struct* 2002;35(8):495–503.
- [8] Shehata MH, Thomas MDA. Use of ternary blends containing silica fume and fly ash to suppress expansion due to alkali-silica reaction in concrete. *Cem Concr Res* 2002;32(3):341–9.
- [9] Thomas MDA, Shehata MH, Shashiprakash SG, Hopkins DS, Cail K. Use of ternary cementitious systems containing silica fume and fly ash on concrete. *Cem Concr Res* 1999;29(8):1207–14.
- [10] Lilkov V, Dimitrova E, Petrov O. Hydration process of cement containing fly ash and silica fume: the first 24 h. *Cem Concr Res* 1997;27(4):577–88.
- [11] Weng JK, Langan BW, Ward MA. Pozzolanic reaction in Portland cement, silica fume, and fly ash mixtures. *Can J Civ Eng* 1997;24(5):754–60.
- [12] Kwan AKH, Wong HHC. Packing density of cementitious materials: part 2 – packing and flow of OPC + PFS + CSF. *Mater Struct* 2008;41(4):773–84.
- [13] Diamond S, Sahu S. Densified silica fume: particle sizes and dispersion in concrete. *Mater Struct* 2006;39(9):849–59.
- [14] Yajun J, Cahyadi JH. Effects of densified silica fume on microstructure and compressive strength of blended cement pastes. *Cem Concr Res* 2003;33(10):1543–8.
- [15] Wolsiefer J Sr. The measurement and analysis of silica fume particle size distribution and de-agglomeration of different silica fume product forms. In: Malhotra VM, editor. Proceedings Ninth CANMET/ACI international conference on fly ash, silica fume, and natural pozzolans in concrete, SP 242. American Concrete Institute, Farmington Hills, Mich; 2007. p. 111–32.
- [16] Bognacki CJ, Pirozzi M, Marsano J, Baumann WC. Rapid chloride permeability testing's suitability for use in performance-based specifications. *Concr Int* 2010;32(5):47–52.
- [17] Ahmed MS, Kayali O, Anderson W. Chloride penetration in binary and ternary blended cement concretes as measured by two different rapid methods. *Cem Concr Compos* 2008;30(7):576–82.
- [18] Shi C. Effect of mixing proportions of concrete on its electrical conductivity and the rapid chloride permeability test (ASTM C1202 or AASHTO T277) results. *Cem Concr Res* 2004;34(3):537–45.
- [19] Hooton RD, Thomas MDA, Stanish K. Prediction of chloride penetration in concrete. Report No. FHWA-RD-00-142. FHWA, US DOT; 2001.
- [20] Radlinski M, Olek J. High-performance concrete bridge decks: a fast-track implementation study. FHWA/IN/JTRP-25/11, Joint transportation research program, vol. 2. Purdue University, West Lafayette, Ind; 2008.
- [21] Berke NS, Hicks MC. Estimating the life cycle of reinforced concrete decks and piles using laboratory diffusion and corrosion data. In: Chaker V, editor. Corrosion forms and control for infrastructure, ASTM STP 1137, ASTM, Philadelphia (Pa); 1992. p. 207–31.
- [22] Bentz DP, Ehlen MA, Ferraris CF, Garboczi E. Sorptivity-based service life predictions for concrete pavements. In: Proceedings 7th international conference on concrete pavement. International society for concrete pavements, vol. 1. Orlando, FL. September 9–13; 2001. p. 181–93.
- [23] Wexham developments. JAF calorimeter operating manual. 4th ed. Reading Berks, UK; 1996.
- [24] Wong HHC, Kwan AKH. Packing density of cementitious materials: part 1 – measurement using a wet packing method. *Mater Struct* 2008;41(4):689–701.
- [25] Goldman A, Bentur A. Bond effects in high-strength silica-fume concretes. *ACI Mater J* 1989;86(5):440–7.
- [26] Kleiner M, Tekkaya AE, Speck K. Development of ultra high performance concrete dies for sheet metal hydroforming. *Prod Eng* 2008;2(2):201–8.
- [27] Tsartsari A, Byars E. Ultra-high-performance concrete using conventional casting. *Concrete* 2002 [January].
- [28] Ballim Y, Graham PC. The effects of supplementary cementitious materials in modifying the heat of hydration of concrete. *Mater Struct* 2009;42(6): 803–11.
- [29] Nocuń-Wczelik W. Fly ash-silica fume-cement paste-kinetics of hydration. In: Malhotra VM, editor. Proceedings Ninth CANMET/ACI international conference on fly ash, silica fume, and natural pozzolans in concrete, SP 242. American Concrete Institute, Farmington Hills, Mich; 2007. p. 249–52.
- [30] Marsch BK, Day RL. Pozzolanic and cementitious reactions of fly ash in blended cement pastes. *Cem Concr Res* 1988;18(2):301–10.
- [31] Yogendran V, Langan BW, Ward MA. Hydration of cement and silica fume paste. *Cem Concr Res* 1991;21(5):691–708.
- [32] Zhang M-H, Gjorv OE. Effect of silica fume on cement hydration in low porosity cement pastes. *Cem Concr Res* 1991;21(5):800–8.
- [33] Lilkov V, Petrov O. Hydration of cement mixed with “Pozzolit” mineral additive. In: Justnes H, editor. Proceedings 10th international congress on the chemistry of cement, vol. 3. Gothenburg, Sweden; June 1997.
- [34] Zelić J, Rušić D, Veža D, Krsulović R. The role of silica fume in the kinetics and mechanisms during the early stage of cement hydration. *Cem Concr Res* 2000;30(10):1655–62.
- [35] Sarkar SL, Balbaaki M, Aitcin P-C. Microstructural development in a high-strength concrete containing a ternary cementitious system. *Cem Concr Agg* 1991;16(2):81–7.
- [36] Lu P, Sun G, Young JF. Phase composition of hydrated DSP cement pastes. *J Am Ceram Soc* 1993;76(4):1003–7.
- [37] Hewlett PC. Lea's chemistry of cement and concrete. Elsevier Ltd.; 1998.
- [38] Young JF, Hansen W. Volume relationships for C-S-H formation based on hydration stoichiometries. *Mater Res Soc Symp Proc* 1987;85:313–22.
- [39] Feldman RF, Ramachandran VS. Differentiation of interlayer and adsorbed water in hydrated Portland cement by thermal analysis. *Cem Concr Res* 1971;1(6):607–20.